

Modification of magnetotransport properties across patterned GaMnAs nanoconstrictions by application of high current densities

Sung Un Cho,¹ Hyung Kook Choi,¹ Chan Uk Yang,¹ Yun Daniel Park,^{1,a)}
 Fabio C. S. Da Silva,² Teresa Osminer,² and David P. Pappas²

¹*Department of Physics and Astronomy, Seoul National University, NS 50, Seoul 151-747, Republic of Korea*

²*National Institute of Standards and Technology, Boulder, Colorado 80305, USA*

(Received 3 April 2009; accepted 18 June 2009; published online 17 July 2009)

We report on modifications in the magnetotransport properties across patterned GaMnAs nanoconstrictions by the application of high current densities ($<10^7$ A/cm²). Initially, we observe controllable changes in the electrical resistance with the direction of the bias current. Repeated biases at high current densities greatly increase the constriction resistances. Subsequent biasing and magnetotransport measurements show nearly a fourfold increase in the magnetoresistances and large changes in the magnetic switching behavior of GaMnAs. The initial reversibility of the changes in resistance suggests that dopant electromigration may locally alter the interstitial concentrations of Mn at the nanoconstriction. © 2009 American Institute of Physics. [DOI: 10.1063/1.3182720]

Carrier-mediated ferromagnetism in GaMnAs-diluted magnetic semiconductors has attracted considerable interest both for fundamental research and in the development of spintronic semiconductor devices.¹ The unique correlations between the magnetic and electronic properties of GaMnAs (Ref. 2) have resulted in the demonstration of unconventional manipulation of its magnetic properties, such as by electric fields³ and strain.⁴ In addition to intrinsic magnetotransport effects such as anisotropic magnetoresistance (AMR) (Ref. 5) and anomalous Hall effect,⁶ phenomena such as spin-dependent scattering⁷ (spin-valve), tunneling⁸ (magnetic tunnel junction), and current-induced domain wall motion⁹ have also been demonstrated in GaMnAs. Likewise, the phenomenon of magnetotransport, particularly spin-dependent transport across a lateral nanoconstriction, has attracted significant attention. In patterned constrictions from ferromagnetic transition metal thin films, there have been several reports^{10–12} of controllably reducing the physical dimensions by the electromigration of metallic ions at high current densities. In GaMnAs, reduction in constriction dimensions is primarily limited by standard nanofabrication processing techniques.^{4,13–15} In this letter, we investigate how applying repeated biases of high current densities can alter the magnetotransport properties across a GaMnAs nanoconstriction.

The Mn ion in GaMnAs is ambipolar depending on whether it is substitutional (Mn_{Ga}) or interstitial (Mn_i). The Mn ion acts as a shallow acceptor or as a deep-level double donor depending on whether it is substitutional or interstitial, respectively. Typically, although a small at. % of Mn is incorporated into the host GaAs matrix, the observed magnetic properties have been attributed to only a fraction of the Mn concentration,² i.e., to those Mn ions that are located at the group III (Ga) site. On the other hand, Mn_i ions as well as Mn–Mn complexes degrade the magnetic properties of GaMnAs. Mn_i is a double donor, which effectively reduces the hole carrier concentration and electrical conductance; in the

case of Mn–Mn complexes, the nearest-neighbor complexes are antiferromagnetically coupled. Nevertheless, researchers have found that annealing as-grown GaMnAs at growth temperatures of approximately 250 °C increases the hole carrier concentration (p) and magnetic ordering temperatures (T_C).¹ Such drastic improvements in p and T_C are thought to be caused by the thermal diffusion of nonsubstitutional Mn ions to the surface of GaMnAs with an energy barrier of 0.7 eV (Refs. 16 and 17). Annealing at temperatures much higher than 250 °C brings about a decrease in both p and T_C , as Mn_{Ga} begins to precipitate, forming nanometer-sized intermetallic MnAs particles.¹⁸ At reduced dimensions such as those found in a nanoconstriction, the effect of self-annealing caused by Joule heating or other mechanisms on the magnetotransport properties have not yet been addressed.

First, we pattern lateral constrictions in GaMnAs nanowires. The geometry of the patterned nanoconstrictions is expected to enhance the current densities and electric fields and act as an efficient pinning site for magnetic domain walls. First, a 100 nm Ga_{1-x}Mn_xAs ($x \approx 0.05$)/50 nm low-temperature (LT)-GaAs buffer/semi-insulating-GaAs (001) substrate is prepared by LT molecular beam epitaxy. The details of this process can be found elsewhere.¹⁹ After growth, GaMnAs nanowires (width: 800 nm and length: 10 μ m) with 20–100 nm nanoconstriction are patterned by e-beam lithography and selective wet chemical etching.¹⁵ The axis of the nanowire is along the [110] direction. A typical scanning electron microscopy (SEM) micrograph of the resulting nanoconstrictions is shown in Figs. 1(a) and 1(b). After the patterning of the nanoconstriction, electrical contacts [Ti (20 nm)/Au (200 nm)] are made to the nanowires using standard photolithography techniques and involving e-beam evaporation and subsequent lift-off. The nanoconstriction devices are wire-bonded and their magnetotransport properties are characterized in a modified commercially available magnetocryostat at 5 K with applied magnetic fields of up to 7 T. The nanowire is biased by a dc current source and the potential across the nanoconstriction is measured using a nanovoltmeter. Figure 1(c) shows the temperature dependence of normalized resistance for various

^{a)} Author to whom correspondence should be addressed. Electronic mail: parkyd@phya.snu.ac.kr.

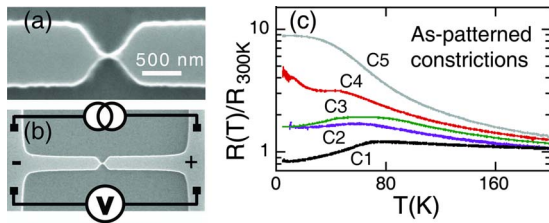


FIG. 1. (Color online) (a) SEM micrograph of GaMnAs wire with nanoconstriction. (b) Schematic illustration of the experimental setup. (c) Normalized resistances as the function of the temperature for various AP nanoconstrictions and the corresponding accompanying Hall bar with $R_{NC}=7$ k Ω (C1: Hall bar), (C2) 12 k Ω , (C3) 31 k Ω , (C4) 60 k Ω , and (C5) 150 k Ω at $T=300$ K.

as-patterned (AP) nanoconstrictions and the corresponding standard Hall bar structure. All temperature dependences in nanoconstriction resistance, except that of the highest resistance, show a local anomaly, a shoulder, near T_C . Although such anomalies have been associated with ferromagnetic “metallic” GaMnAs (Ref. 2), it is not clear whether absence of such anomalies indicate such AP nanoconstrictions as nonmagnetic. Nevertheless, we will now concentrate on nanoconstrictions that show local peak in temperature dependence of resistance near T_C .

GaMnAs nanoconstrictions are biased similar to that in a feedback-controlled electromigration process.²⁰ Since the resistivity of GaMnAs ($\rho \approx 5$ m Ω cm at $T=5$ K) is several orders of magnitude higher than that of metals, the current rather than voltage is specified and varied. At cryogenic temperatures ($T=5$ K), the bias current is slowly increased while the voltage drop across the nanoconstriction is monitored. Initial current bias (I_B) sweeps (duration: <60 s) are accompanied by changes in nanoconstriction resistances (R_{NC}). The bias current for a particular nanoconstriction is limited to a current value (I_B^{Max}) a posteriori depending on the initial R_{NC} value. At this point, the bias current is lowered and then increased again to I_B^{Max} . The resulting changes in resistance across the nanoconstriction (ΔR_{NC}) of a representative sample are plotted as a function of a series of I_B sweeps [Fig. 2(a)]. The values of I_B^{Max} vary from

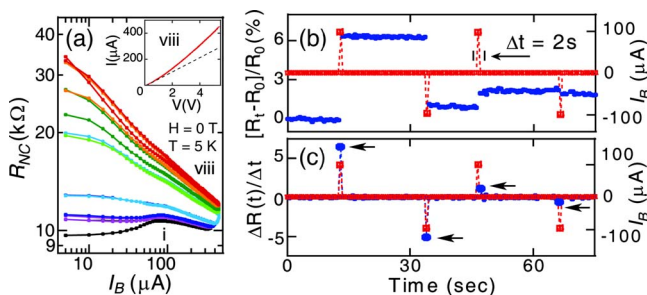


FIG. 2. (Color online) (a) Observed R_{NC} values as functions of I_B for a series of eight current bias sweeps at $T=5$ K and $H=0$ T. Small Roman numerals indicate the n^{th} bias current sweep ($I_B:0 \rightarrow I_B^{\text{Max}} \rightarrow 0$). The inset shows a nonlinear IV response after the eighth current bias sweep (dotted line depicts a ohmic response as a guide). (b) Percentage change in resistance (solid circle) across another nanoconstriction is observed for bias current (open square) applied for a duration of 2 s at $T=5$ K. The relative change in resistance ($I_r=1$ μ A) across the nanoconstriction (ΔR_{NC}) coincides with the applied bias currents ($I_B = \pm 100$ μ A). (c) Plot of $DR(t)/dt$ for the values mentioned in (b). For the first duration ($I_B = +100$ μ A), $[\Delta R(t)/\Delta t] > 0$. During the second duration ($I_B = -100$ μ A), $[\Delta R(t)/\Delta t] < 0$. Successive dependences of ΔR_{NC} on the direction of the bias current are found to become weaker.

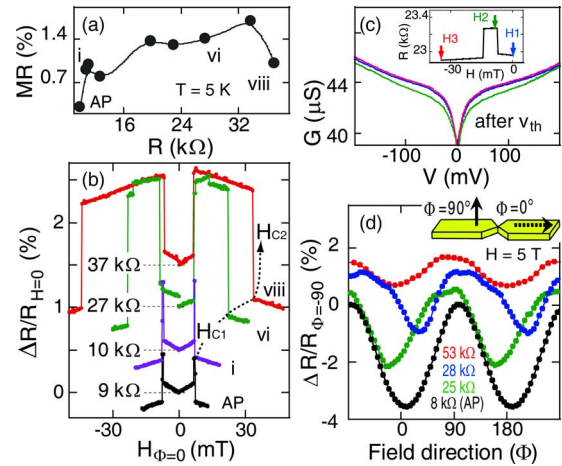


FIG. 3. (Color online) (a) $MR = [R_{NC}(H) - R_{NC}(0)]/R_{NC}(0)$ as a function of the R_{NC} for the nanoconstriction depicted in Fig. 2(a) shows a marked decrease for $R_{NC} > 30$ k Ω . (b) MR measured at $T=5$ K for AP and after first (i), sixth (vi), and eighth (viii) current bias sweeps. Increases in H_{C2} with successive current bias sweeps are highlighted by the dotted line. (c) Calculated dI/dV (conductance) as a function of the bias current across the nanoconstriction at $T=5$ K after the fifth current bias sweep for various applied magnetic fields (inset). (d) Angular dependence of MR for another nanoconstriction at 5 T after various bias current sweeps. The curves are offset for clarity.

50–1000 μ A (or $J_B^{\text{Max}} < 10^7$ A/cm²) depending on the initial R_{NC} value. For the nanoconstriction depicted, R_{NC} at low bias increases by more than threefold (from $R_{NC} < 10$ k Ω to $R_{NC} > 30$ k Ω). Initially, nanoconstriction resistances (R_{NC}) are nearly independent with bias, but after several repeated bias sweeps, nonlinear I - V characteristic becomes more evident with $dR_{NC}/dI_B < 0$ [Fig. 2(a) inset].

We can estimate an upper-bound change in the local temperature ($\Delta T_{NC} < 50$ K $< T_C$) in terms of joule heating effects by comparing $\Delta R_{NC}/R_{NC}$ with the resistance as a function of temperature before applying I_B^{Max} . Furthermore, to determine whether the initial changes in R_{NC} can be attributed to self-annealing, which is caused by joule heating effects, we perform the following experiment. We apply $\pm I_B^{\text{Max}}$ (50 and 100 μ A) for 2 s durations at $T=5$ K and measure R_{NC} with a reading current (I_r) of 1 μ A ($< 0.02 I_B^{\text{Max}}$) [Figs. 2(b) and 2(c)]. We observe a relative change in resistance, which depends on the direction of bias current. We find that $\Delta R_{NC} > 0$ for a particular bias direction and that $\Delta R_{NC} < 0$ for the opposite bias direction. Although the dependence of ΔR_{NC} on the direction of the bias current reduces after several pulses, such behavior cannot be solely attributed to self-annealing, which is caused by joule heating effects (i.e., increase in ΔR_{NC} cannot be solely attributed to Mn_{Ga} precipitation as such process is irreversible).

In addition to ΔR_{NC} , relative changes in Mn concentration near the nanoconstriction affect the magnetotransport properties, particularly the magnetic switching characteristics and MR values. In an extreme case, nanocrystalline MnAs impurities have been found to increase the magnetic coercivity of GaMnAs (Ref. 21). Thus, at $T=5$ K between successive sweeps of I_B^{Max} [Fig. 2(a)], we conduct magnetotransport measurements with $I_r=3$ μ A and under an applied magnetic field of $\leq \pm 5$ T along the axis of the nanowire. Reproducible increases in the MR ratio $\{MR = [R_{NC}(H) - R_{NC}(0)]/R_{NC}(0)\}$ are observed when R_{NC} is increased up to ~ 30 k Ω [Figs. 3(a) and 3(b)]. In the case of a

particular nanoconstriction, we observe a nearly fourfold increase in MR (with MR of 0.5% for AP and 1.7% after tenth bias current sweep). As R_{NC} approaches 25.8 k Ω ($\approx h/e^2$), i.e., the tunneling regime, the MR ratio begins to decrease [Fig. 3(a)]. After a series of bias sweeps, along with an increase in MR, a large increase in $H_{\text{C}2}$ is observed [Fig. 3(b)]. As mentioned previously, nonlinear I - V characteristics and their applied magnetic field dependence are noted [Fig. 3(c)].

A similar dependence of R_{NC} on MR and an angular dependence¹¹ [Fig. 3(d)] have been reported in Permalloy ($\text{Ni}_{0.8}\text{Fe}_{0.2}$) break junctions,¹⁰ although the exact mechanisms underlying these dependencies are most likely different. In contrast, the switching behavior as a function of R_{NC} differs considerably in GaMnAs nanoconstrictions. The AMR response across the GaMnAs constriction deteriorates after successive sweeps to I_B^{Max} , possibly due to successive increases in defect concentrations within the junction. Furthermore, the magnetic switching behavior in Permalloy break junctions reflects the shape anisotropy of the Permalloy leads of differing dimensions. Here, initially the magnetotransport measurements of the AP nanoconstrictions indicate small differences between the magnetic coercivities ($H_{\text{C}1}$ and $H_{\text{C}2}$) of the left and right leads, as expected; these differences are due to small nonintentional differences in the lead dimensions. After successive bias sweeps, large differences between $H_{\text{C}1}$ and $H_{\text{C}2}$ are found, such behavior may be explained in terms of differences in Mn concentration across the nanoconstriction.

Increases in R_{NC} , MR, and $H_{\text{C}2}$, which are due to the repeated application of high bias currents at 5 K, cannot be solely attributed to Joule heating effects. Even at the above-mentioned current densities, it is not possible to fully attribute Joule heating effects for long-term increases in R_{NC} since the local temperature at the nanoconstriction is significantly lower than the temperature at which Mn_{Ga} is expected to readily precipitate. Such an increase in R_{NC} would also result in degradation of the magnetotransport properties, particularly MR. Another reason for the changes in R_{NC} is thought to be the relative change in the $\text{Mn}_{\text{Ga}}/\text{Mn}_{\text{I}}$ concentrations, similar to those observed during low-temperature annealing studies. The increase in MR and the changes in $H_{\text{C}2}$ can be attributed to the relative changes in Mn_{I} concentration. The long-term increase in R_{NC} may be explained on the basis of the defects generated due to the migration of the Mn_{I} ions facilitated by vacancy defects. Transition metal-doped semiconductors have been modeled as mixed electronic-ionic conductors, and the transition metal ion diffusion phenomenon influenced by a driving force is well-studied.²² Analogous to the Mn ions in GaAs, substitutional Cu ions (with $r_{\text{Cu}^{2+}}/r_{\text{Mn}^{2+}} \approx 1$) can also act as immobile acceptors while Cu_{I} ions act as donors. Depth profiling carried out to detect ^{64}Cu in n -GaAs reveals a clear shift in the profile of ^{64}Cu due to the applied electric field attributable to dopant electromigration of Cu_{I} ions.²³

In summary, we have shown that the resistance across a GaMnAs nanoconstriction undergoes controllable and reversible changes, initially. From the results of magnetotransport measurements, we found considerable improvements in MR values even with accompanying increases in R_{NC} and marked increases in the magnetic switching fields up to the

R_{NC} that corresponds to the tunneling regime. However, the changes observed cannot be solely attributed to the effects of self-annealing due to joule heating effects. We believe that dopant electromigration at the nanoconstriction might have played an important role in the changes observed in magnetotransport properties. Thus, further studies are required to study this effect in more detail.

This study was primarily supported by the Seoul R&BD Program. S.U.C. acknowledges the support extended by the Seoul Science Fellowship program. Y.D.P. acknowledges the support from NRF Nano R&D Program funded by the Ministry of Education, Science, and Technology (2008-02795). Contribution of the US Government is not subject to copyright.

- ¹A. H. MacDonald, P. Schiffer, and N. Samarth, *Nature Mater.* **4**, 195 (2005).
- ²T. Jungwirth, J. Sinova, J. Masek, J. Kucera, and A. H. MacDonald, *Rev. Mod. Phys.* **78**, 809 (2006).
- ³H. Ohno, D. Chiba, F. Matsukura, T. Omiya, E. Abe, T. Dietl, Y. Ohno, and K. Ohtani, *Nature (London)* **408**, 944 (2000).
- ⁴K. Pappert, S. Humpfer, C. Gould, J. Wenisch, K. Brunner, G. Schmidt, and L. W. Molenkamp, *Nat. Phys.* **3**, 573 (2007).
- ⁵A. W. Rushforth, K. Vyborny, C. S. King, K. W. Edmonds, R. P. Campion, C. T. Foxon, J. Wunderlich, A. C. Irvine, P. Vasek, V. Novak, K. Olejnik, J. Sinova, T. Jungwirth, and B. L. Gallagher, *Phys. Rev. Lett.* **99**, 147207 (2007).
- ⁶S. H. Chun, Y. S. Kim, H. K. Choi, I. T. Jeong, W. O. Lee, K. S. Suh, Y. S. Oh, K. H. Kim, Z. G. Khim, J. C. Woo, and Y. D. Park, *Phys. Rev. Lett.* **98**, 026601 (2007).
- ⁷G. Xiang, B. L. Sheu, M. Zhu, P. Schiffer, and N. Samarth, *Phys. Rev. B* **76**, 035324 (2007).
- ⁸M. Tanaka and Y. Higo, *Phys. Rev. Lett.* **87**, 026602 (2001); D. Chiba, Y. Sato, T. Kita, F. Matsukura, and H. Ohno, *ibid.* **93**, 216602 (2004).
- ⁹M. Yamanouchi, D. Chiba, F. Matsukura, and H. Ohno, *Nature (London)* **428**, 539 (2004).
- ¹⁰K. I. Bolotin, F. Kuemmeth, A. N. Pasupathy, and D. C. Ralph, *Nano Lett.* **6**, 123 (2006).
- ¹¹K. I. Bolotin, F. Kuemmeth, and D. C. Ralph, *Phys. Rev. Lett.* **97**, 127202 (2006).
- ¹²A. Sokolov, C. Zhang, E. Y. Tsybmal, J. Redepening, and B. Doudin, *Nat. Nanotechnol.* **2**, 171 (2007).
- ¹³C. Rüster, T. Borzenko, C. Gould, G. Schmidt, L. W. Molenkamp, X. Liu, T. J. Wojtowicz, J. K. Furdyna, Z. G. Yu, and M. E. Flatté, *Phys. Rev. Lett.* **91**, 216602 (2003).
- ¹⁴A. D. Giddings, M. N. Khalid, T. Jungwirth, J. Wunderlich, S. Yasin, R. P. Campion, K. W. Edmonds, J. Sinova, K. Ito, K. Y. Wang, D. Williams, B. L. Gallagher, and C. T. Foxon, *Phys. Rev. Lett.* **94**, 127202 (2005).
- ¹⁵S. W. Cho, H. K. Choi, J. S. Lee, D. Jeong, H. J. Kim, T. Hwang, K. H. Kim, and Y. D. Park, *Appl. Phys. Lett.* **91**, 122514 (2007).
- ¹⁶K. W. Edmonds, P. Boguslawski, K. Y. Wang, R. P. Campion, S. N. Novikov, N. R. S. Farley, B. L. Gallagher, C. T. Foxon, M. Sawicki, T. Dietl, M. B. Nardelli, and J. Bernholc, *Phys. Rev. Lett.* **92**, 037201 (2004).
- ¹⁷J. Masek and F. Maca, *Phys. Rev. B* **69**, 165212 (2004).
- ¹⁸H. K. Choi, Y. S. Kim, S. S. A. Seo, I. T. Jeong, W. O. Lee, Y. S. Oh, K. H. Kim, J. C. Woo, T. W. Noh, Z. G. Khim, Y. D. Park, and S. H. Chun, *Appl. Phys. Lett.* **89**, 102503 (2006).
- ¹⁹Y. S. Kim, I. T. Jeong, J. C. Woo, Z. G. Khim, J. S. Lee, H. K. Choi, Y. S. Oh, K. H. Kim, Y. D. Park, and S. H. Chun, *J. Korean Phys. Soc.* **47**, 306 (2005).
- ²⁰D. R. Strachan, D. E. Smith, D. E. Johnston, T. H. Park, M. J. Therien, D. A. Bonnell, and A. T. Johnson, *Appl. Phys. Lett.* **86**, 043109 (2005).
- ²¹K. Y. Wang, M. Sawicki, K. W. Edmonds, R. P. Campion, A. W. Rushforth, A. A. Freeman, C. T. Foxon, B. L. Gallagher, and T. Dietl, *Appl. Phys. Lett.* **88**, 022510 (2006).
- ²²D. Cahen and L. Chernyak, *Adv. Mater. (Weinheim, Ger.)* **9**, 861 (1997).
- ²³R. N. Hall and J. H. Racette, *J. Appl. Phys.* **35**, 379 (1964).